

## Angle-resolved photoemission from epitaxial $\text{YBa}_2\text{Cu}_3\text{O}_{7-x}$ (001) films

Y. Sakisaka, T. Komeda, T. Maruyama, and M. Onchi

*Department of Chemistry, Faculty of Science, Kyoto University, Kyoto 606, Japan*

H. Kato

*Photon Factory, National Laboratory for High Energy Physics, Tsukuba-shi, Ibaraki 305, Japan*

Y. Aiura and H. Yanashima

*Institute of Physics, University of Tsukuba, Tsukuba-shi, Ibaraki 305, Japan*

T. Terashima and Y. Bando

*Institute for Chemical Research, Kyoto University, Uji 611, Japan*

K. Iijima, K. Yamamoto, and K. Hirata

*Research Institute for Production Development, Kyoto 606, Japan*

(Received 11 October 1988)

Angle-resolved photoemission from epitaxially grown  $\text{YBa}_2\text{Cu}_3\text{O}_{7-x}$  (001) single-crystal thin films reveals a clear Fermi edge and fine structure near the edge. Some of the valence-band photoemission features show  $k$ -space dispersion. These new results suggest that the electronic structure of this oxide can be treated within the framework of the one-electron band picture.

Since the recent discovery of superconductivity above 90 K in  $\text{YBa}_2\text{Cu}_3\text{O}_{7-x}$  (Y-Ba-Cu-O),<sup>1</sup> numerous studies have been made in order to determine the mechanism responsible. As yet, however, there is no confirmed theory. Detailed knowledge of the electronic structure is important for understanding the mechanism. A number of angle-integrated photoemission experiments on sintered pellets of this oxide<sup>2</sup> have been done to explore the density of occupied states and show disagreement between observed and calculated<sup>3-7</sup> spectra and the importance of electron-correlation effects, supporting Anderson's starting point.<sup>8</sup> However, a major problem in the study of sintered materials is the quality of the sample. Scraping with a diamond file to prepare a fresh surface may destroy the compound selvage.<sup>9</sup> Furthermore, angle integration smears fine structure near the Fermi energy ( $E_F$ ). Recently, Stoffel *et al.*<sup>10</sup> reported an angle-resolved photoemission spectroscopy (ARUPS) study of cleaved single-crystal samples. Unfortunately, they found no clear Fermi edge. This paper reports an ARUPS study of epitaxial Y-Ba-Cu-O (001) films at 300 K. Our data show the normal-state Fermi edge, fine structures near  $E_F$ , and dispersion effects on some of the valence bands.

The ARUPS experiments were performed at the Photon Factory as described elsewhere.<sup>11</sup> The angular resolution was  $\pm 1^\circ$  and the total energy resolution was 0.1–0.2 eV depending on the photon energies ( $h\nu$ ) of 23–60 eV. Baking of the ARUPS chamber was done at  $\sim 80^\circ\text{C}$  to prevent loss of oxygen from the sample. The pressure in the system was in the  $10^{-9}$  Torr range. After all the ARUPS measurements, the cleanness of the surface was confirmed by Auger spectroscopy<sup>12</sup> and its crystalline order by low-energy electron diffraction (LEED). The LEED patterns<sup>12</sup> at 60–100 eV showed sharp spots with a low background which reflect the nearly square two-

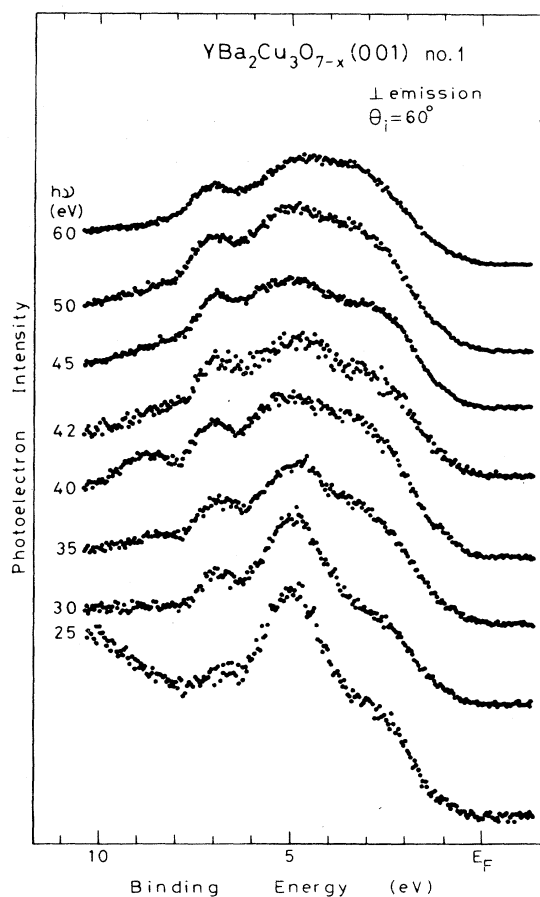


FIG. 1. Normal-emission spectra of the  $\text{YBa}_2\text{Cu}_3\text{O}_{7-x}$  (001) sample No. 1 measured at  $\theta_i = 60^\circ$  for various  $h\nu$ . Data were normalized to the relative flux of incident photons.

dimensional (2D) Brillouin zone (BZ) of the (001) face. All the measurements were made at 300 K and on two separate samples of single-crystal Y-Ba-Cu-O (001) thin films ( $\sim 1000$  Å thick) which were prepared epitaxially on SrTiO<sub>3</sub>(001) substrates as described in Ref. 13. In the ARUPS chamber, the samples were annealed at  $\sim 600^\circ\text{C}$  for  $\sim 20$  min in  $\sim 100$  Torr O<sub>2</sub> and then cooled very slowly. Finally, a few days later, the superconducting transition was checked and the endpoint of the dc-resistive transition [ $T_c(R=0)$ ] occurred at 88 K with a transition width  $\Delta T$  (10%-90%) of  $\sim 1.5$  K (the resistivity at 290 K was  $\sim 200$   $\mu\Omega$  cm) as before.<sup>14</sup>

The calculated valence-band structures of Y-Ba-Cu-O previously reported<sup>3-7</sup> are similar to one another except for the details. The valence-band structure comes from a complex set of 36 bands and, therefore, it is impossible to observe each band separately even by ARUPS. However, we note rather simple band structures near the top ( $E_F$ ) and bottom and a large band gap (or an area of low density of states) at  $\sim 2$ -3 eV below  $E_F$  at  $M$  (we use the same symmetry labels as in Refs. 4 and 7).

Figure 1 shows normal-emission spectra of the Y-Ba-Cu-O (001) sample No. 1 measured at a light incidence angle of  $\theta_i = 60^\circ$  from the surface normal and at various

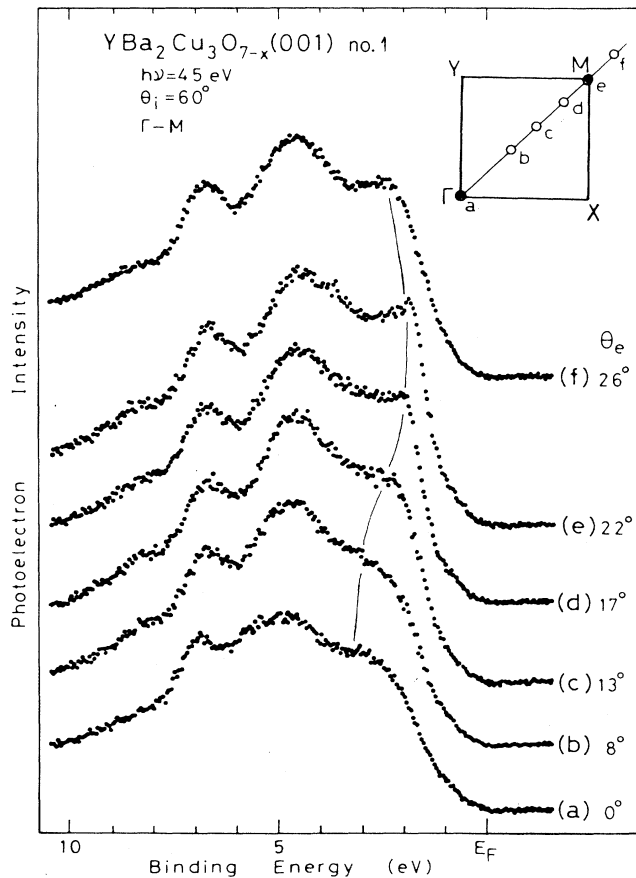


FIG. 2. Off-normal emission spectra of the YBa<sub>2</sub>Cu<sub>3</sub>O<sub>7-x</sub> (001) sample No. 1 along  $\Gamma$ - $M$  measured at  $h\nu = 45$  eV and  $\theta_i = 60^\circ$ , and at various emission angles  $\theta_e$  from the surface normal.

$h\nu$ . Four major features are seen at  $\sim 3$ ,  $\sim 5$ ,  $\sim 7$ , and  $\sim 8.5$  eV. These features do not move within  $\pm 0.2$  eV with  $h\nu$ , in agreement with the highly two-dimensional (2D) nature of the band structure. The 8.5-eV feature appears only at  $h\nu \sim 40$  eV and may be due to an umklapp process involving the reciprocal-lattice vector  $\mathbf{G}(110)$ . This feature differs from a feature previously observed at 9-10 eV in the spectra of the sintered materials<sup>2</sup> and in Ref. 10, because the 9-10 eV feature, which has been attributed to H<sub>2</sub>O or OH<sup>-</sup> species,<sup>15</sup> becomes weak with increasing  $h\nu$  (e.g., from 26 to 180 eV).<sup>2,15</sup> With increasing  $h\nu$  from 25 to 60 eV, only the 5-eV feature becomes weak, leading us to identify it as most likely O-derived bands.

Figure 2 shows off-normal spectra for sample No. 1 taken at  $h\nu = 45$  eV and  $\theta_i = 60^\circ$  along  $\Gamma$ - $M$ . Similar spectra for No. 2 are shown in Fig. 3 ( $h\nu = 40$  eV,  $\theta_i = 25^\circ$ ,  $\Gamma$ - $M$ - $\Gamma_2$ ). The position in  $k$  space Brillouin zone (BZ) where each spectrum probes is also indicated. The 5- and 7-eV features stay at almost fixed locations as  $k$  is changed, while the 3-eV feature at  $k = 0$  ( $\Gamma$ ) disperses to lower binding energy with increasing  $k$  from  $\Gamma$  to  $M$  ( $\sim 2$  eV at  $M$ ) and, thereafter, to higher-binding energy. Along  $\Gamma$ - $M$ - $\Gamma$  the dispersion of the 3-eV feature is periodic about the  $M$  point. Notice that at  $\Gamma$  in the second zone, the spectrum in Fig. 3 returns to that at  $\Gamma$  in the first zone. Thus, the dispersion of the 3-eV feature exhibits the

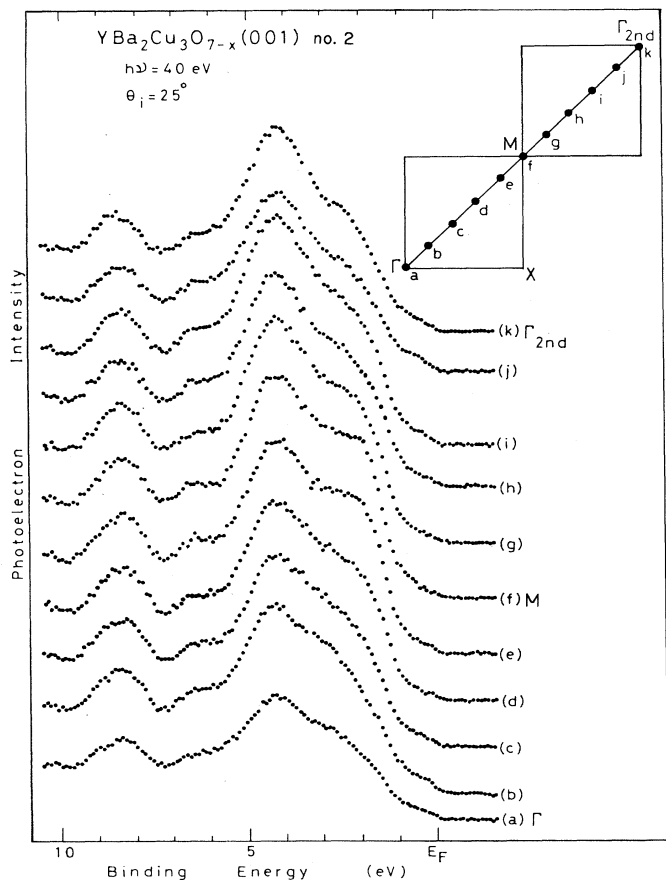


FIG. 3. As Fig. 2 but for sample No. 2,  $h\nu = 40$  eV, and  $\theta_i = 25^\circ$  (along  $\Gamma$ - $M$ - $\Gamma_2$ ).

correct periodicity for a  $(1 \times 1)$  structure. A large valley at  $\sim 3$  eV (or a large separation between the 3- and 5-eV features) seen in the spectra (*f*) at *M* can be considered to reflect the large band gap (or the area of low density of states) in the range  $\sim 2$  to  $\sim 3.5$  eV at around *M* in the calculated band structures.<sup>3,5-7</sup> A direct comparison between observed and calculated structures is impossible without the calculated *k*-resolved density of states. However, the band calculations<sup>3,5,6</sup> indicate that the upper main bands in the first  $\sim 1$  eV above the "gap" exhibit relatively large dispersion along  $\Gamma$ -*X*-*M* as compared with the lower ones in the first  $\sim 1$  eV below the "gap," which is in consistency with our data. For example, Ref. 3 shows that the upper main bands disperse from  $\sim 2.5$  eV at  $\Gamma$  to  $\sim 1.1$  eV at *M* ( $\sim 1.4$ -eV dispersion), while the lower ones disperse from  $\sim 3.2$  eV at  $\Gamma$  to  $\sim 3.8$  eV at *M* ( $\sim 0.6$ -eV dispersion). Figure 2 shows that the 8.5-eV feature is visible away from  $\Gamma$  and most pronounced at around *M*. We cannot decide from our data whether this result is related to dispersion effects or simply to varying peak intensity. Reference 7 predicts the bottom band at  $\sim 8.5$  eV at *M*. The positions of the observed "gap" and peaks do not agree with any band calculation (except for Ref. 7). The energy shift required for agreement is

$\sim 0.5$ – $1$  eV. However, we note that the correspondence between experiment and calculation is improved when the calculated bandwidth in Refs. 3–6 is expanded by 20%–30%.

The dispersive nature of the valence bands is also seen for the states near  $E_F$ . Figure 4 shows off-normal spectra for sample No. 1 in the Fermi-edge region measured at  $h\nu = 40$  eV and  $\theta_i = 25^\circ$  along  $\Gamma$ -*X*-*M*- $\Gamma$ . Similar spectra for No. 2 measured at  $h\nu = 23$  eV and  $\theta_i = 60^\circ$  are shown in Fig. 5. The position in *k* space (BZ) where each spectrum probes is also indicated. Fine structures (marked by triangles) are clearly seen in the region between 0.5 and 1 eV from  $E_F$  in Figs. 4 and 5, respectively. Each of the observed features in Fig. 4 has a counterpart in Fig. 5. The noise level and the energy resolution of 0.15 eV at  $h\nu = 40$  eV and 0.1 eV at  $h\nu = 23$  eV are small enough to observe such features, the lifetime broadening effects of which are very small in the Fermi-edge region. The important result is the observation of a clear Fermi edge in spectra (*b*), (*f*), (*j*), and (*r*) in Fig. 4 and some spectra in Fig. 5. The existence of a Fermi surface means that each one-electron wave vector *k*, a good quantum number, in *k* space. Furthermore, the fine structures disperse with *k* and some of them

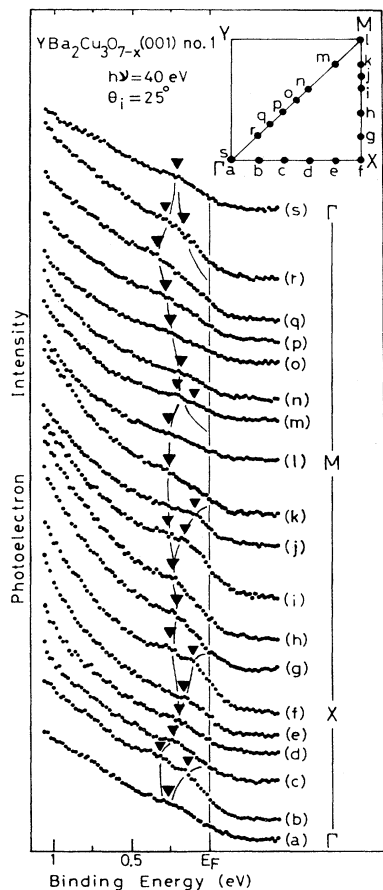


FIG. 4. Off-normal emission spectra of the  $\text{YBa}_2\text{Cu}_3\text{O}_{7-x}$  (001) sample No. 1 along  $\Gamma$ -*X*-*M*- $\Gamma$  measured at  $h\nu = 40$  eV and  $\theta_i = 25^\circ$ .

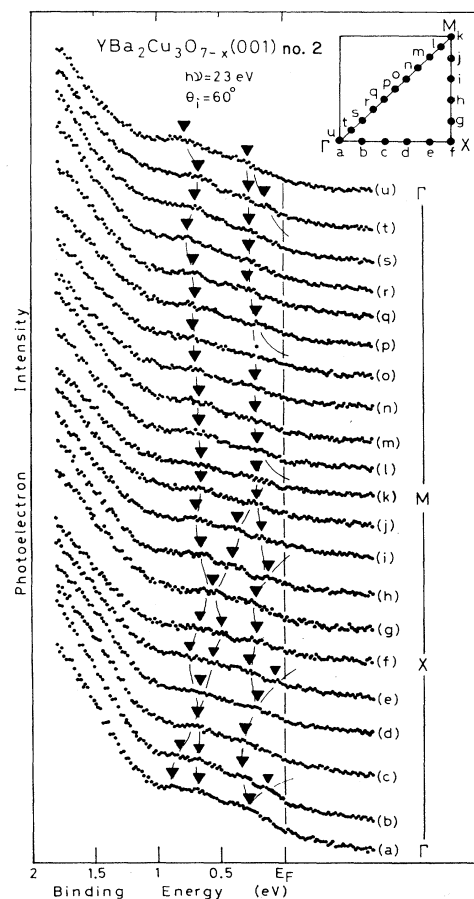


FIG. 5. As Fig. 4 but for sample No. 2,  $h\nu = 23$  eV, and  $\theta_i = 60^\circ$ .

look to cross  $E_F$ . The possible dispersion of these features is tentatively indicated by thin solid lines in each figure, which can be compared with the calculated band structures in Refs. 3–6. For example, Ref. 4 shows that the bands cross  $E_F$  near  $\Gamma$  along  $\Gamma$ - $X$  (band 1 along  $\Gamma$ - $Y$  in Ref. 3), near  $X$  (band 4 near  $Y$  in Ref. 3), in the midpoint between  $X$  and  $M$  (bands 2 and 3 along  $Y$ - $S$  in Ref. 3), near  $M$  and  $\Gamma$  along  $M$ - $\Gamma$ , which is in consistency with our data. The complexity of deep-lying bands between  $\sim 0.5$  and 1 eV makes it hard to compare with the observations. However, we note that the band structure along  $\Gamma Y$  of Ref. 3 shows two pairs of bands starting at 0.4 eV and  $\sim 0.7$  eV from  $\Gamma$ , in agreement with our data.

In summary, our ARUPS data indicate that the elec-

tronic structure of Y-Ba-Cu-O is compatible with band theory, but do not necessarily rebut the importance of electron-correlation effects, which are already strong in any ordinary metals. The previous studies of a valence-band satellite in Ni showed that the band model is a reasonable approximation for the ground state and the additional electron correlations of the excited state can be treated within perturbation theory.<sup>16</sup>

We are pleased to thank the staff of the Photon Factory, National Laboratory for High Energy Physics, for their excellent support. This work has been performed under the approval of the Photon Factory Program Advisory Committee (Proposal No. 88-U-002).

<sup>1</sup>C. W. Chu *et al.*, Phys. Rev. Lett. **58**, 405 (1987); R. J. Cava *et al.*, *ibid.* **58**, 1676 (1987).

<sup>2</sup>A. Samsavar *et al.*, Phys. Rev. B **37**, 5164 (1988), and references therein.

<sup>3</sup>S. Massidda *et al.*, Phys. Lett. A **122**, 198 (1987); J. Yu *et al.*, *ibid.* **122**, 203 (1987).

<sup>4</sup>L. F. Mattheiss and D. R. Hamann, Solid State Commun. **63**, 395 (1987).

<sup>5</sup>G. Zhao *et al.*, Phys. Rev. B **36**, 7203 (1987).

<sup>6</sup>B. Szpunar and V. H. Smith, Phys. Rev. B **37**, 7525 (1988).

<sup>7</sup>B. A. Richert and R. E. Allen, Phys. Rev. B **37**, 7869 (1988).

<sup>8</sup>P. W. Anderson, Science **235**, 1196 (1987).

<sup>9</sup>F. P. Bowden and D. Tabor, *The Friction and Lubrication of Solids* (Oxford Univ. Press, Oxford, 1956); M. Fink and D.

Hofman, Z. Metallkd. **3**, 24 (1932).

<sup>10</sup>N. G. Stoffel *et al.*, Phys. Rev. B **37**, 7952 (1988). Note that their sample had the very wide transition width  $\Delta T$  (10–90%) of  $\sim 40$  K.

<sup>11</sup>H. Kato *et al.*, Phys. Rev. B **32**, 1992 (1985); *ibid.* **34**, 8973 (1986).

<sup>12</sup>Y. Sakisaka *et al.* (unpublished).

<sup>13</sup>T. Terashima *et al.*, Jpn. J. Appl. Phys. **27**, L91 (1988).

<sup>14</sup>The superconducting properties of the thin films thus prepared were kept at 300 K even in vacuum for at least 1–2 weeks, except for heating in vacuum at above  $\sim 150$  °C.

<sup>15</sup>Q. L. Qiu *et al.*, Phys. Rev. B **37**, 3747 (1988).

<sup>16</sup>G. Treglia, F. Ducastelle, and D. Spanjaard, J. Phys. (Paris) **43**, 341 (1982), and references therein.